



European Geosciences Union General Assembly 2014, EGU 2014

## A Diagnostic diagram to understand atmosphere-ocean dynamics in the southern North Sea at high wind speeds

Anthony J. Kettle\*

*Geophysical Institute, University of Bergen, P.O. Box 7803, Bergen 5020, Norway*

---

### Abstract

Long time series of offshore meteorological measurements in the lower marine atmospheric boundary layer show dynamical regimes and variability that are forced partly by interaction with the underlying sea surface and partly by the passage of cloud systems overhead. At low wind speeds, the dynamics and stability structure of the surface layer depend mainly on the air-sea temperature difference and measured wind speed at a standard height. The physical processes are mostly understood and quantified through Monin-Obukhov (MO) similarity theory. At high wind speeds, different dynamical regimes become dominant, with breaking waves, sea spray, and organized boundary layer convection cells contributing to observed effects. Data from offshore meteorological monitoring sites typically show different behavior and regime shifts depending on the local winds and synoptic conditions. However, the regular methods to interpret time series through spectral analysis only give a partial view of the dynamics in the atmospheric boundary layer. Wind speed and the air-sea temperature difference are important factors that characterize the dynamics of the lower atmospheric boundary layer, and they provide a dynamic and thermodynamic constraint to frame observed processes, especially at high wind speeds. Early studies of long time series of automated offshore meteorological data recognized the value of the joint probability distribution on axes of wind speed and air-sea temperature difference to summarize large segments of the data. The approach can be extended to probe the marine atmospheric boundary layer conditions that are important for the loading of offshore wind turbines: turbulence intensity and wave conditions. The increasing numbers of offshore meteorological masts that are associated with the offshore wind industry are amenable to a similar approach to understand the main characteristics of the boundary layer. In this case, the diagnostic figure provides a method to ‘fingerprint’ the atmospheric conditions at an offshore site.

© 2014 The Authors. Published by Elsevier Ltd. This is an open access article under the CC BY-NC-ND license (<http://creativecommons.org/licenses/by-nc-nd/3.0/>).

Peer-review under responsibility of the Austrian Academy of Sciences

*Keywords:* similarity theory; FINO1; Frøya database; Staffjord A; North Sea.

---

\* Corresponding author. Tel.: +47 5583259; fax: +47 55589883.  
*E-mail address:* [ake043@gf.uib.no](mailto:ake043@gf.uib.no)

## 1. Introduction

The development of offshore wind energy has brought to light important gaps in understanding of dynamical and thermodynamic processes in the marine atmospheric boundary layer especially in coastal regions. Meteorological flows at all heights are characterized by a complexity that is imperfectly understood and difficult to simulate numerically, and this is partly because of physical interactions that interact across a wide range of time and space scales ranging from microscopic aerosol scales up to mesoscale and planetary dimensions. Numerical simulation difficulties arise in particular regions of the atmosphere where small and large scale circulation processes interact, and one important area is the marine atmospheric boundary layer (MABL) in coastal areas. Here, there are complicated interactions between the ocean wave field and the overlying atmosphere, with additional considerations of shallow bathymetry, internal boundary layers in the atmosphere, and the effect of cloud interactions at the top of the MABL. Offshore wind energy is focusing development on coastal regions, which hold important advantages compared with onshore sites: higher wind speeds for energy extraction and lower average turbulence intensity to limit fatigue damage of turbines. However, the meteorological complexity of coastal oceanographic zones is not completely understood. Partly, this is because coastal meteorology has not been intensively investigated in the past, and the high meteorological masts (~100m) that the wind industry is erecting for offshore resource assessment have revealed unexpected dynamical features with implications for the fatigue loading of turbines.

The most important geophysical parameters relevant to the operation and the licensing of offshore wind turbines are encapsulated in the industry standard IEC 64100-3 (2009) [1] guidelines, which were developed from a combination of onshore wind turbine guidelines and offshore standards from the oil and gas industry for seabed foundations [2]. At its core, the objective of the guidelines is to address factors related to the ultimate failure and fatigue loading of offshore wind turbines, which are important to assess how the turbine structure survives in storm winds and also how minor structural damage accrues from repeated loading from the wind turbulence and waves. From the meteorological perspective, certain key measurements and diagnostics are highlighted for the operation of offshore wind turbines over the 20 year design lifetime. After the assessment of the hub-height wind speed for resource assessment, the quantification of turbulence levels is important. This is given by the diagnostic quantity ‘turbulence intensity’ (TI) or the ratio of the standard deviation to the mean wind speed for an extended high resolution time series. The TI parameter is used directly in numerical simulations to calculate turbine fatigue loads [3] and hence has an important ranking among measured geophysical parameters for site assessment. Other important parameters are related to extreme conditions: for example the extreme 3 second gust and 10 minute wind speed with a 50 year return period.

Ocean conditions are treated differently within the IEC61400-3 guidelines and reflect the fact that the support structure will necessarily be constructed according to the local site conditions, which must be assessed with an onsite survey. The most important ocean conditions for support structure loading are the wave field and ocean currents. The wave field is described according to the summary statistics: significant wave height, peak spectral period, and mean wave direction. The wave climate at an offshore site depends on wind speed [2]. However, the relation among these parameters is characterized by a significant level of scatter, and this is mostly due to the additional importance of fetch and water depth [4]. Other important ocean factors within the IEC61400-3 guidelines include sea currents, water level, marine growth, and scour [2], but meteorologically-forced wave effects are highlighted as an important factor to assess fatigue loading.

The consideration of both atmospheric and oceanic factors in turbine load considerations creates a multidimensional problem that is difficult to conceptualize. Additional factors arise from the choice of averaging time scale for any given geophysical measurement, which potentially adds extra dimensionality to the problem [5]. Current practice within the offshore industries is to visualize data as a scatter diagram projection in two dimensional space. However, for surface wave forecasting, this is particularly difficult as the basic problem to determine significant wave height depends on considerations of wind speed, wind duration, and fetch [4]. For both meteorological and oceanographic load considerations, the most important geophysical factors are wind speed and atmospheric stability, which is accounted in a number of different ways, of which the simplest is the difference between air and sea surface temperature. From the meteorological viewpoint, atmospheric stability is important because it determines the turbulence intensity and vertical shear that are experienced across the turbine rotor area. From the oceanographic viewpoint, wind speed and atmospheric stability are also important for determining the

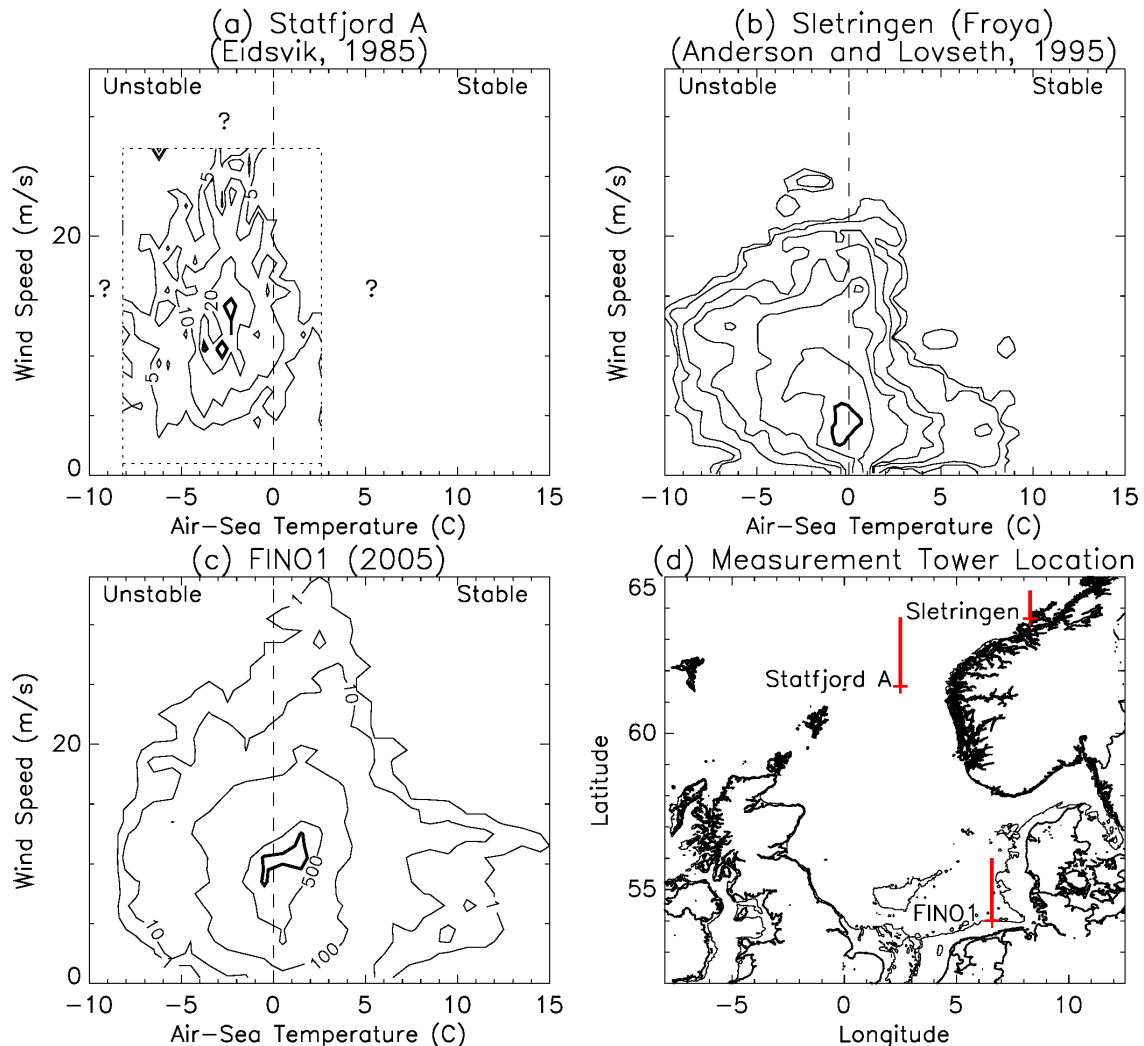


Fig. 1. Joint probability distribution of wind speed versus air-sea temperature difference for (a) Statfjord A (June 1979–April 1982) [19], (b) Sletringen coastal site (February 26, 1988–May 15, 1989) [20], and (c) FINO1 North Sea measurement tower (January 1–December 31, 2005), and (d) map with location of meteorological sites with coastline (<http://shoreline.noaa.gov/data/datasheets/wvs.html>) and 30 m isobath from ETOPO1 (<http://www.ngdc.noaa.gov/mgg/global/global.html>). The ‘?’ symbols in (a) denote missing information in the truncated tabular format of Eidsvik (1985) [19].

surface wave field, since the communication of wind momentum from the atmospheric to the upper ocean and wave fields depends partly on atmospheric stratification.

The objective of this contribution is to use a diagnostic diagram based on wind speed and air-sea temperature difference (abbreviated as the ‘V- $\Delta$ T diagram’) to investigate important factors in offshore turbine design: turbulence intensity and surface wave field. The approach is to reduce a complicated time series of met-ocean parameters into a phase space defined by a kinetic factor (wind speed) and a simple thermodynamic factor (air-sea temperature difference).–

## 2. Background

The importance of wind speed and atmospheric stability in determining the dynamical properties of the atmospheric boundary layer was recognized from the earliest MABL investigations. Taylor (1914, 1917) [6,7] tabulated underway research cruise data from the northeast Atlantic Ocean to link fog frequency in the MABL with

conditions of air-sea temperature difference and wind speed. Woodcock (1940) [8] was the first to explicitly use the V- $\Delta$ T diagram to explain the flying patterns of the herring gulls, illustrating how large scale thermal plumes over the ocean represent an importance process for the vertical exchange of heat and momentum through the MABL. The importance of wind speed and atmospheric stability for radar propagation over the ocean was intensively researched during World War II in extended campaigns off the west coast of Wales [9] and Massachusetts Bay [10]. A variant of V- $\Delta$ T diagram appeared in a summary report of the U.S. work to explain statistical trends in the multi-year time series that had been collected near the end of the war [10]. Investigations from the 1940's through to the 1980's linked cloud patterns over open ocean areas with wind speed and air-sea temperature difference [11,12,13]. Coastal air pollution studies from 1970's-1980's employed the V- $\Delta$ T diagram to interpret tracer dispersion results [14,15]. The diagram been invoked to explain the role of atmospheric stability on vertical wind profile features [16,17]. The fundamental importance of V- $\Delta$ T diagram for sea air turbulent fluxes of water vapor, temperature, and momentum, was highlighted by Smith (1988) [18], who modified the air temperature criterion to include water vapour buoyancy effects (i.e. virtual temperature).

In offshore wind energy, the V- $\Delta$ T diagram was an important way to gain an overview of MABL characteristics in two long-term wind speed offshore surveys in northwest Europe in areas of the North and Norwegian Seas that were targeted for energy resource development. Eidsvik (1985) [19] reported on a high-quality multi-year time series of wind speed measured at 110 m height at the top of the Statfjord A offshore platform in the Norwegian Sea. Andersen and Løvseth (1995) [20] presented a time series of wind speeds measured on a 45 m high meteorological mast at Sletringen at a coastal region near Trondheim, Norway. Both meteorological studies were linked with industrial projects in high wind locations and aimed to achieve a statistical description of offshore meteorological conditions that could adversely impact safety and operations. To get an overview of the information and geophysics, the V- $\Delta$ T diagram was an important element of the early analysis (replotted in Fig. 1a and b, together with measurement locations Fig. 1d). While the two sites have broadly similar characteristics in the V- $\Delta$ T diagrams, there are features that serve to fingerprint and differentiate the main wind speed resource and turbulent load characteristics of the sites. Most notably, meteorological conditions at Statfjord A were characterized by higher wind speeds with a narrower range of variability with the predominance of unstable atmospheric stability conditions. Open questions remain about the distribution of other important geophysical quantities on the axes represented by the V- $\Delta$ T diagram: turbulence intensity and the surface wave field.

### 3. FINO1 Data Set

Data from the FINO1 offshore research platform are used to extend the analysis from a joint probability distribution to a tool to understand important met-ocean conditions. The FINO1 measurement tower was built in 2003 to support a German government initiative for background meteorological information to support offshore wind farm construction and operation, part of a policy to shift the base of the country's power production from fossil fuels and nuclear technologies to renewables [21]. The tower is well instrumented with an array of 8 Vector-100 cup anemometers on booms that extend from the southeast corner of the mast at ~10 m intervals from 33–100 m height. Three Gill sonic anemometers (at 40, 60, and 80 m height) are located on booms that extend from the northwest corner of the mast. Wind direction information is provided by a Thies wind vane at 90 m height at northwest edge of the mast and is important for assessing mast shadow effects. The mast has an array of air temperature sensors at 30, 40, 50, 70, and 100 m. The 30 m air temperature measurement is used in this report along with an upper ocean temperature measurement time series from 2 m depth (Sea and Sun temperature sensor) to assess atmospheric static stability. A Waverider Wave-C buoy was moored several hundred meters northwest of the platform in 2005, and this provided summary statistics of the sea state in the form of significant wave height, peak period, and wave direction. Most data were downloaded from the BSH website where they are provided as 10 minute average quantities (or 30- and 60-minutes summary statistics for the Wave-C buoy.) The 10Hz sonic anemometer data for 2005 were provided by F. Kinder of the Deutsches Windenergie Institut (DEWI GmbH).

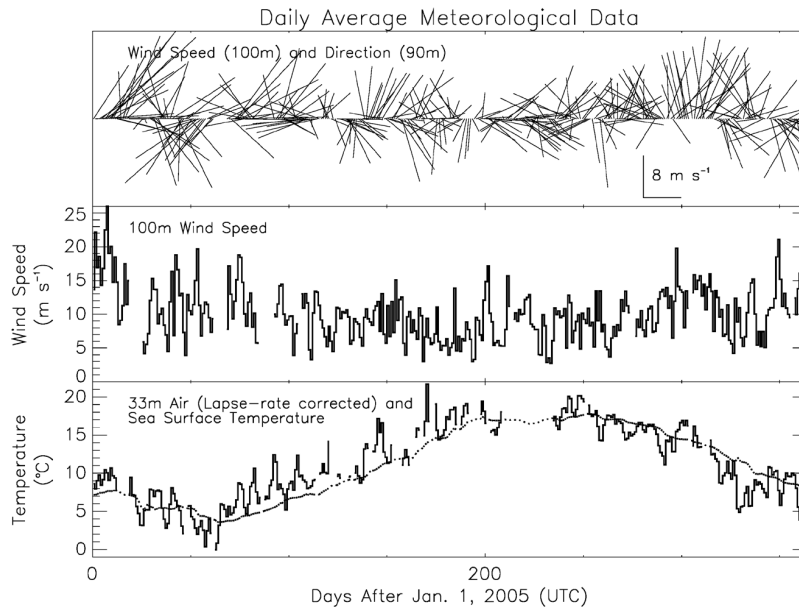


Fig. 2. Day average values of (a) wind speed (100 m) and direction (90 m), (b) magnitude of wind speed (100 m), and air (solid line) and near surface sea (dotted line) temperature at FINO1.

A summary time series for the 2005 FINO1 time series is shown in Fig. 2. The diagram illustrates the high data availability at this early stage of the FINO1 program and the seasonal progression of meteorological conditions at the site. Winds are predominantly from southwest and highest in winter. Air temperatures are mainly warmer than sea temperatures (stable atmospheric conditions) in the early summer and cooler than sea temperatures (unstable atmospheric conditions) in the autumn and early winter. The time series diagram gives limited information about the relation between wind speed and air-sea temperature difference, but the corresponding  $V-\Delta T$  diagram (Fig. 1c) highlights the relative frequency different meteorological the conditions that impact the loading of offshore wind structures for this site.

### 3.1. Turbulence Intensity (TI)

For the FINO1 2005 data, the TI has been calculated from the 80 m sonic anemometer data, and the bin average is shown as a joint probability distribution in the  $V-\Delta T$  diagram in Fig. 3a. The mast-impacted wind direction sector  $100-152^\circ$  has been excluded from the analysis. Dotted lines of bulk Richardson number have been overplotted on the diagram to highlight the dynamical mixing regimes at this offshore location, and particularly the onset of mechanical mixing during stable atmospheric conditions. The figure shows the important impact that atmospheric stability has on TI. For comparison, Fig. 3b shows a conventional presentation of bin-average TI versus wind speed, similar to the type that is used by the wind industry for turbine loading assessments (see <http://winddata.com>). The information in Fig. 3b is based on measured data collected on the FINO1 tower from 2003–2007 [22,23]. The figure shows typical TI conditions at offshore locations with higher values nearer the sea surface from surface wave effects, and a characteristic minimum inflection at intermediate wind speeds of  $\sim 10$  m/s, depending on the instrument measurement height above sea level. The advantage of the  $V-\Delta T$  diagram is that it highlights the important role of air-sea temperature difference in determining TI. In particular, serious TI conditions arise where high winds and conditions of large atmospheric instability occur together.

TI can vary over a large range of values for a given wind speed, and its statistical distribution at a given wind speed is characterized by a high degree of skewness [5]. Because of the way that the construction materials of offshore turbine structures accrue fatigue damage in response to higher orders of wind speed [3], higher statistical moments of TI are particularly important. Fig. 3c therefore presents the minimum and maximum TI values for a

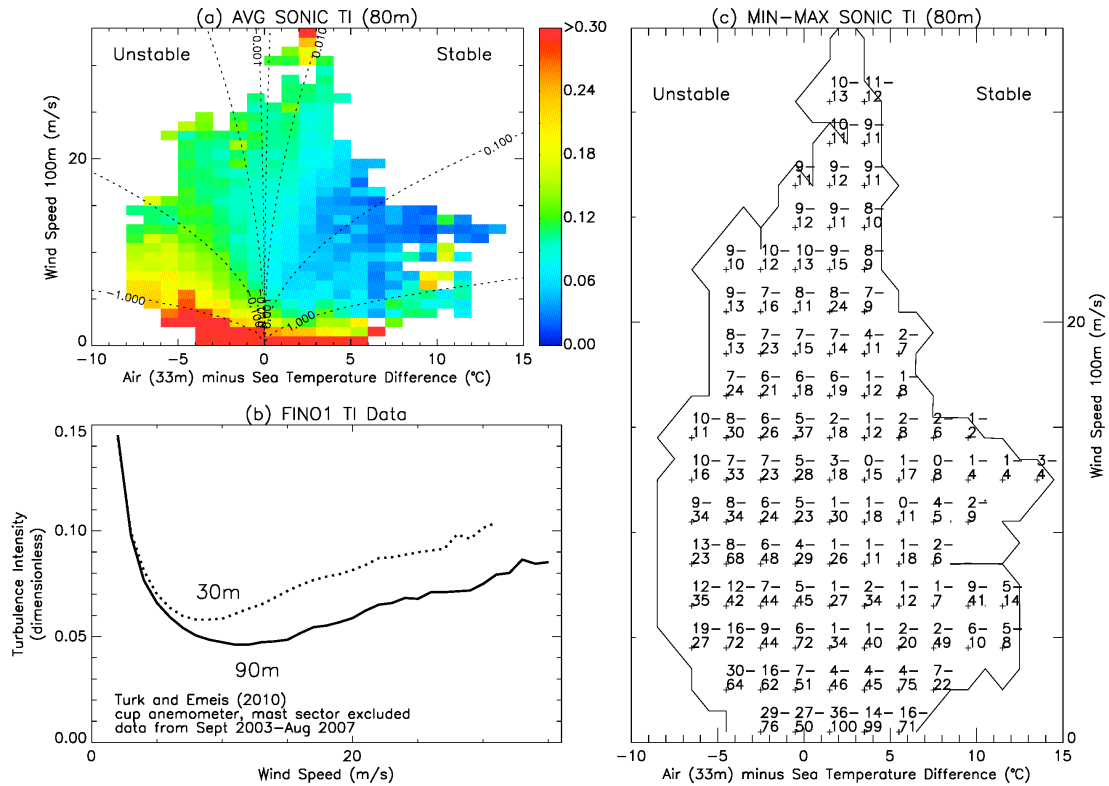


Fig. 3. (a) Turbulence intensity from the 80 m sonic anemometer plotted as bin averages on axes of wind speed (100 m) versus air temperature (33 m height) minus sea temperature (2 m depth); (b) turbulence intensity from FINO1 at 30 m and 90 m height digitized from [23]; (c) as for Fig. 3a but showing the bin minimum- maximum range of turbulence intensities (expressed as a percentage) on an extended wind speed axis with an outline of the joint probability distribution for orientation.

subset of the bins in the  $V-\Delta T$  diagram. The figure highlights that the envelope of maximum measured TI from the sonic anemometer may be significantly higher than the IEC 61400-3 guidelines.

### 3.2. Surface Wave Field

The occurrence of severe storms at FINO1 has caused structural damage on at least three occasions during different winter storms ([24,25,26], <http://www.fino1.de/meldungen/alle-meldungen/137-15-meter-welle-beschaedigt-fino1>). This initiated research to understand the link between the wind and wave field during storm conditions. It is normal practice in the offshore industry to represent wave climate in terms of a wave scatter table of significant wave height versus period ([4], <http://www.globalwavestatisticsonline.com>). Fig. 4a shows such a table for the FINO1 wave buoy for 2005. The diagram shows the range of significant wave heights that have been recorded for a full annual cycle at this location in the German Bight, and the upper envelope of the distribution is related to a wave field that is growing in contact with the overlying wind. However, the figure only gives a partial information about the sea state, which also depends on wind speed, fetch (i.e., distance to the nearest upwind coast), and atmospheric stability. Probing the relationship between sea state and wind speed during two winter storm episodes, [27] present an analysis of significant wave height versus wind speed (similar to Fig. 4b). They concluded that there is a relationship between the two parameters but that is complicated by additional factors wind direction, atmospheric stability and fetch. Winter storms in the German Bight have a different character depending on if the

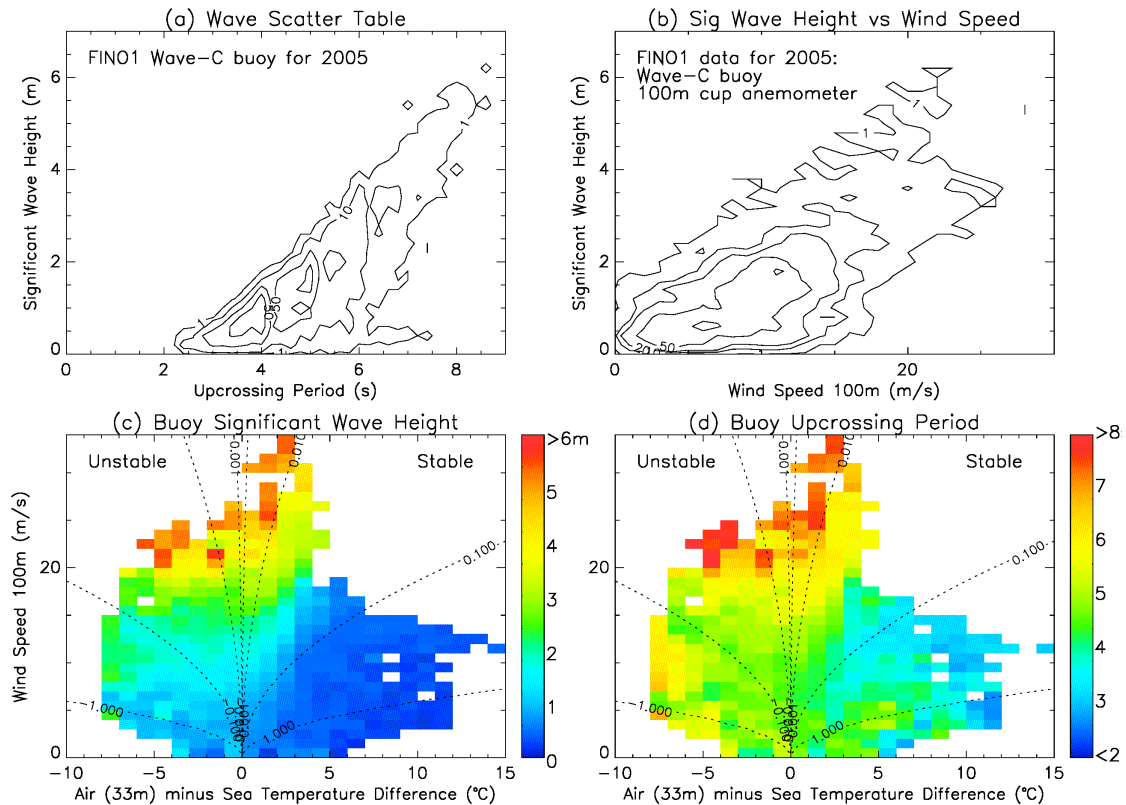


Fig. 4. (a) Contoured wave scatter table of significant wave height versus upcrossing period, (b) significant wave height versus 100 m wind speed, (c) bin-average significant wave height on axes of wind speed (100 m) versus air temperature (33 m height) minus sea temperature (2 m depth), (d) as for Fig.3c but with bin-averages of upcrossing period.

wind is from the west with short fetch and stable atmospheric conditions (e.g., storm ‘Erwin’, Jan. 8, 2005) or from the north with long fetch and unstable atmospheric conditions (e.g., storm ‘Britta’, Nov. 1, 2006).

To illustrate the importance of atmospheric stability, Fig. 4c shows average significant wave height on the  $V-\Delta T$  joint probability distribution diagram. The figure is clearly asymmetrical across the line of  $0^{\circ}\text{C}$  air-temperature difference, and unstable conditions are associated with larger the significant wave heights compared stable conditions. Large scale eddy circulation through the MABL in the unstable case facilitates the downward propagation of momentum from the atmosphere to the upper ocean. In the stable atmospheric regime, there is a partial coupling of atmospheric layers from the sea surface that may persist for wind speeds up to 20 m/s [22,23]. The wave period in the  $V-\Delta T$  of figure 4d shows broadly similar conditions as significant wave height.

#### 4. Conclusion

Atmospheric boundary layer dynamics over the ocean depends strongly on wind speed and air-sea temperature difference, and a number of meteorological investigations have highlighted the importance of this parameter set in the  $V-\Delta T$  diagram. In many cases, published investigations have used the  $V-\Delta T$  diagram for a joint probability distribution as part of a statistical survey of long time series, and this has been used to good effect in offshore energy applications [19, 20]. However, the  $V-\Delta T$  diagram is also important as a diagnostic for other met-ocean parameters that are significant for offshore operations. In this contribution, statistical summaries of TI and significant wave height for the FINO1 platform in the German Bight have been plotted on the  $V-\Delta T$  diagram to highlight the importance of atmospheric stability. These parameters are particularly important for the offshore wind industry for

assessing loads on offshore turbines. Many coastal locations in northwest Europe have been identified as potential sites for wind farm development. While different locations may have broadly similar resource the potential as identified from a wind atlas, the details of wind characteristics as revealed in the V- $\Delta$ T diagram serve to differentiate and fingerprint different sites and improve understanding of turbine loading and lifetime.

## Acknowledgements

Part of the data in this analysis is from the research project FINO (research platforms in the North Sea and Baltic Seas), which is funded by BMU, the Germany Federal Ministry for the Environment, Nature Conservation and Nuclear Safety. This work has been performed as part of the Norwegian Centre for Offshore Wind Energy (NORCOWE) under grant 193821/S60 funded by the Research Council of Norway (RCN).

## References

- [1] IEC61400-3. Wind Turbines – Part 3: Design requirements for offshore wind turbines. International Electrotechnical Commission; 2009.
- [2] Quarton DC. An international design standard for offshore wind turbines: IEC 61400-3, [http://wind.nrel.gov/public/SeaCon/Proceedings/Copenhagen.Offshore.Wind.2005/documents/papers/Design\\_basis/D.Quarton\\_An\\_international\\_design\\_standard\\_for\\_offshore.pdf](http://wind.nrel.gov/public/SeaCon/Proceedings/Copenhagen.Offshore.Wind.2005/documents/papers/Design_basis/D.Quarton_An_international_design_standard_for_offshore.pdf); 2005.
- [3] Eliassen L, Jakobsen JB, Ohrai C. The effect of atmospheric stability on the fatigue life of offshore wind turbines. Proceedings of the Twenty-second (2012) International Offshore and Polar Engineering Conference, Rhodes, Greece, June 17-22, 2012, International Society of Offshore and Polar Engineers (ISOPE); 2012.
- [4] WMO-No.702. Guide to wave analysis and forecasting. World Meteorological Organization; 1998.
- [5] Morales A, Wachter M, Peinke J. Characterization of wind turbulence by higher order statistics. *Wind Energy* 2012;15:391-406.
- [6] Taylor GI. Mr. Taylor's report, Report on the work carried out by the S.S. Scotia, 1913. Ice observation, meteorology, and oceanography in the North Atlantic Ocean. H.M. Stationary Office, London; 1914.
- [7] Taylor GI. The formation of fog and mist. *Quarterly Journal of the Royal Meteorological Society* 1917;43:241-268.
- [8] Woodcock AH. Convection and soaring over the open sea. *Journal of Marine Research* 1940;3:248-253.
- [9] Sheppard PA. The structure and refractive index of the lower atmosphere. Meteorological Factors in Radio-Wave Propagation. Report of a Conference held on 8 April 1946 at The Royal Institution, London, The Physical Society, London; 1946. p. 37-79.
- [10] Craig RA, Katz I, Montgomery RB, Rubenstein PJ. Chapter 3. Meteorology of the Refraction Problem. In Kerr DE, editor. *Propagation of Short Radio Waves*. McGraw-Hill Book Company, New York; 1951. p. 181-293.
- [11] Woodcock AH, Wyman J. Convective motion in air over the sea. *Annals of the New York Academy of Sciences* 1947;48:749-776.
- [12] Kuettner J. The band structure of the atmosphere. *Tellus* 1959;2:267-294.
- [13] Agee EM, Sheu PJ. MCC and gull flight behaviour. *Boundary Layer Meteorology* 1978;14:247-251.
- [14] Schacher GE, Fairall CW, Zannetti P. Comparison of stability classification methods for parameterizing coastal overwater dispersion. First International Conference on Meteorology and Air/Sea Interaction of the Coastal Zone. May 10-12, 1982, The Hague, Netherlands, American Meteorological Society and Royal Netherlands Meteorological Institute; 1982.
- [15] Hsu SA. An overwater stability criterion for the offshore and coastal dispersion model. *Boundary Layer Meteorology* 1992;60:397-402.
- [16] Roll UU. *Physics of the Marine Atmosphere*. Academic Press, New York; 1965.
- [17] Hsu SA, Meindl EA, Gilhousen DB. Determining the power-law wind-profile exponent under near-neutral stability conditions at sea. *Journal of Applied Meteorology* 1994;33:757-765.
- [18] Smith SD. Coefficients for sea surface wind stress, heat flux, and wind profiles as a function of wind speed and temperature. *Journal of Geophysical Research* 1988;93:15467-15472.
- [19] Eidsvik KJ. Large-sample estimates of wind fluctuations over the ocean. *Boundary-Layer Meteorology* 1985;32:103-132.
- [20] Anderson OJ, Løvseth J. Gale force maritime wind. The Frøya data base. Part 1: Sites and instrumentation. Review of the data base. *Journal of Wind Engineering and Industrial Aerodynamics* 1995;57: 97-109.
- [21] Rehfeldt K, Paschedeig U, Bomer J. Offshore wind power development in Germany. BMU, Stiftung der deutschen Wirtschaft zur Nutzung und Erforschung der Windenergie auf See, Jan.; 2007.
- [22] Türk M. Ermittlung designrelevanter Belastungsparameter für Offshore-Windkraftanlagen, Ph.D. Thesis, Köln; 2008.
- [23] Türk M, Emeis S. The dependence of offshore turbulence intensity on wind speed. *Journal of Wind Engineering and Industrial Aerodynamics* 2010;98:466-471.
- [24] Herklotz K. Oceanographic results of two years operation of the first offshore wind research platform in the German Bight – FINO1. *DEWI Magazin* Nr. 30, Februar; 2007. p.47-51.
- [25] Outzen O, Herklotz K, Heinrich H, Lefebvre C. Extreme waves at FINO1 research platform caused by storm 'Tilo' on 9 November 2007. *DEWI Magazin* No. 33, August; 2008. p. 17-23.
- [26] Pleskachevsky AL, Lehner S, Rosenthal W. Storm observations by remote sensing and influences of gustiness on ocean waves and on generation of rogue waves. *Ocean Dynamics* 2012;62:1335-1351.
- [27] Emeis S, Türk M. Wave-driven wave heights in the German Bight. *Ocean Dynamics* 2009;59:463-475.